Molecular Genetics and Metabolism Reports 45 (2025) 101275

Contents lists available at ScienceDirect

Molecular Genetics and Metabolism Reports

journal homepage: www.elsevier.com/locate/ymgmr

Profiling glycosphingolipid changes in mouse and human cellular models of lysosomal free sialic acid storage disorder

Marya S. Sabir [a,b], Kostantin Dobrenis [c], Allisandra K. Rha [d], Laura Pollard [e], Petcharat Leoyklang [f], Mariah Marrero [c], Carla Ciccone [f], Mary E. Hackbarth [a], Marjan Huizing [f], Raymond Y. Wang [g,h], William A. Gahl [f], Frances M. Platt [i,**], May Christine V. Malicdan [a,f,*]

[a] UDP Translational Laboratory, NIH Undiagnosed Diseases Program, National Human Genome Research Institute, National Institutes of Health, Bethesda, MD, USA
[b] NIH Oxford-Cambridge Scholars Program, University of Oxford, Oxford, UK
[c] Dominick P. Purpura Department of Neuroscience, Rose F. Kennedy Intellectual and Developmental Disabilities Research Center, Albert Einstein College of Medicine, Bronx, NY, USA
[d] Research Institute, Children's Hospital of Orange County, Orange, CA, USA
[e] Biochemical Genetics Laboratory, Greenwood Genetic Center, Greenwood, SC, USA
[f] Human Biochemical Genetics Section, Medical Genetics Branch, National Human Genome Research Institute, National Institutes of Health, Bethesda, MD, USA
[g] Division of Metabolic Disorders, Children's Hospital of Orange County Specialists, Orange, CA, USA
[h] Department of Pediatrics, University of California-Irvine School of Medicine, Irvine, CA, USA
[i] Department of Pharmacology, University of Oxford, Oxford, UK

ARTICLE INFO

Keywords:
Salla disease
Sialin
Gangliosides
Neuraminidase
Mouse embryonic fibroblasts
HEK-293 T

ABSTRACT

Free sialic acid storage disorder (FSASD) is an autosomal recessive lysosomal storage disease caused by biallelic pathogenic variants in *SLC17A5*, which encodes the lysosomal sialic acid transporter, sialin. FSASD is characterized by excessive lysosomal free sialic acid accumulation, leading to either a severe, early-onset lethal phenotype or a progressive neurodegenerative course. To characterize biochemical alterations in FSASD models, we performed comprehensive profiling of glycosphingolipids (GSLs), including sialylated species (i.e., gangliosides), in mouse embryonic fibroblasts (MEFs) derived from Slc17a5-R39C/R39C and Slc17a5-KO/KO mouse models, as well as in human SLC17A5-deficient HEK-293 T cells generated via CRISPR-Cas9-mediated non-homologous end joining. HPLC-based analyses demonstrated GM3 ganglioside accumulation in MEFs and significant reductions in a-series GSLs—including GM2, GM1a, and GD1a—in SLC17A5-deficient HEK-293 T cells. Analysis of neuraminidase 1/3/4 activities revealed consistently elevated activity across all cell models, while cytosolic neuraminidase 2 showed only a modest increase in Slc17a5-R39C/R39C MEFs. Preliminary quantification showed elevated free sialic acid across all models, consistent with the characteristic biochemical defect observed in FSASD and supporting their relevance for mechanistic studies. These findings highlight that free sialic acid storage leads to changes in GSL homeostasis in FSASD mouse (MEFs) and human (SLC17A5-deficient HEK-293T) cellular models, underscoring their utility as models for studying FSASD pathogenesis.

1. Introduction

Lysosomal free sialic acid storage disorder (FSASD) is an ultra-rare neurodegenerative disease caused by biallelic pathogenic variants in *SLC17A5* [1,2], which encodes sialin, a transporter for sialic acid and other acidic sugars [3–6]. Defective sialin activity leads to the accumulation of unconjugated "free" sialic acid in lysosomes, resulting in a range of clinical manifestations. FSASD includes three clinical subtypes: infantile FSASD (MIM#269920), intermediate severe FSASD, and attenuated FSASD (MIM#604369; also known as Salla disease); the latter is characterized by homozygosity for the p.Arg39Cys variant [2,7]. Approximately 250 individuals with FSASD have been reported globally, with 75 % harboring the Finnish founder missense variant, *SLC17A5* c.115C > T (p.Arg39Cys), in homozygous (most common) or compound heterozygous states, while the remainder carry other biallelic variants [7–9]. Genotype-phenotype correlations have been reported in

* Correspondence to: M.C.V. Malicdan, 10 Center Drive - MSC 1851 Building 10, Room 10C103, Bethesda, MD 20892-1851, USA.
** Correspondence to: F. Platt, Department of Pharmacology, University of Oxford, Mansfield Road, Oxford OX1 3QT, UK.
E-mail addresses: frances.platt@pharm.ox.ac.uk (F.M. Platt), maychristine.malicdan@nih.gov (M.C.V. Malicdan).

https://doi.org/10.1016/j.ymgmr.2025.101275
Received 13 August 2025; Received in revised form 4 November 2025; Accepted 4 November 2025

this disorder [2,8,10,11].

Historically, skin-derived fibroblasts from individuals with FSASD have been extensively utilized as in vitro models to investigate the underlying pathophysiological mechanisms of the disorder, providing valuable insights into its molecular etiology [12,13]. Fibroblast-based studies have demonstrated alterations in the turnover of sialoglycoproteins and gangliosides (i.e., sialylated glycosphingolipids (GSLs)) in FSASD, with some studies reporting elevated lysosomal enzyme activities, although this finding has not been consistently observed across all reports [12,14–19]. Recently, two FSASD mouse models—one a knock-out [20,21] and the other a knock-in ([22]; unpublished results [23])—were generated to facilitate more robust analyses. Due to their versatility, rapid growth, and ease of isolation, primary mouse embryonic fibroblasts (MEFs) are widely used as a standard model for functional characterization of gene knock-outs and signaling pathways, as well as in co-culture systems [24,25]. MEFs have also been employed to study autophagy [26], a process that is impaired in FSASD due to defective lysosomal remodeling [27]. To date, FSASD-derived MEFs have not been evaluated with regard to their regulation of GSL/ganglioside metabolism in the context of sialin deficiency.

Glycosphingolipids, including gangliosides, are essential components of the plasma membrane in eukaryotic cells, playing key roles in regulating various cellular processes, both directly and indirectly [28–31]. During membrane turnover, GSLs are routed to the lysosome for degradation by specific hydrolases [32,33]. Mutations in glycohydrolases or their cofactors disrupt GSL catabolism, leading to a group of lysosomal disorders known as glycosphingolipidoses, which often manifest as progressive neurodegenerative diseases due to the high concentration of GSLs in the central nervous system [34–36]. We have also recently reported a significant elevation in ganglioside levels in the CSF of individuals affected with FSASD [37]. However, basic studies on GSL metabolism in FSASD are limited, with previous research in human fibroblasts demonstrating impaired ganglioside turnover [12,19].

In this study, we aimed to advance our understanding of FSASD pathomechanisms by characterizing cellular and biochemical phenotypes in *SLC17A5*-deficient models. Specifically, we investigated potential alterations in GSL metabolism in MEFs from both the *Slc17a5* knock-out model [20,21] and the knock-in model harboring the common p.Arg39Cys variant ([22], unpublished results [23]), as well as in immortalized SLC17A5-deficient HEK-293T cells generated using CRISPR-Cas9-mediated non-homologous end joining (NHEJ) for comparative analyses. We investigated GSL abundance using two highly sensitive and quantitative normal-phase HPLC assays. We also quantified the activity of two lysosomal glycohydrolases, neuraminidase (i.e., sialidase) and β-hexosaminidase via 4-MU-based assays. Neuraminidase is critical for sialic acid metabolism, as it catalyzes the cleavage of terminal sialic acid residues [38], while β-hexosaminidase is involved in the degradation of the ganglioside GM2 [39], a substrate shown to exhibit altered levels in Slc17a5-KO/KO MEFs in our study. Preliminary analyses, conducted with a limited sample size, involved quantifying free and total sialic acid across all cell lines. Collectively, our results reveal disruptions in GSL homeostasis in these cellular models, providing insights into the pathophysiological processes that may contribute to FSASD as well as measurable phenotypes for future therapeutic studies, including gene correction.

2. Materials and methods

2.1. Generation, validation, and culturing of cell models

Primary mouse embryonic fibroblasts (MEFs) were derived and cryopreserved from Slc17a5-R39C/R39C knock-in, Slc17a5-KO/KO knock-out, and corresponding wild-type embryos using standardized dissociation protocols. HEK293T cells were subjected to CRISPR-Cas9–mediated genome editing to generate SLC17A5-deficient clones, with biallelic frameshift mutations confirmed via Sanger sequencing. Additionally, primary human fibroblast lines, including one derived from a clinically diagnosed intermediate severe FSASD patient, were maintained under defined culture conditions for downstream biochemical analyses. Detailed experimental procedures for all cell models are provided in Supplementary Methods and Methods.

2.2. Quantifying Slc17a5/SLC17A5 gene expression in cells

For quantitative RT-PCR, total RNA was extracted using the Qiagen RNeasy Mini Kit (cat# 74106) according to the manufacturer's instructions. Reverse transcription was performed using the Applied Biosystems High-Capacity RNA-to-cDNA™ Kit (cat# 4387406) in a 20 μL reaction volume per sample, consisting of 10 μL 2× RT buffer mix, 1 μL 20× RT enzyme mix, nuclease-free water, and 2000 ng of RNA, with water volumes adjusted based on sample concentrations.

In the MEFs, quantitative RT-PCR was performed in a 10 μL reaction volume. Each reaction contained 5 μL of 2× TaqMan Gene Expression Master Mix (Applied Biosystems, cat# 4369016), 0.5 μL of 20× TaqMan Gene Expression Assay (*Hprt* (Mm03024075_m1), *Slc17a5* Exon 2–3 boundary (Mm00555337_m1), and *Slc17a5* Exon 10–11 boundary (Mm00555344_m1)), 1 μL of cDNA (25 ng), and 3.5 μL of RNase-free water. Negative template controls were included by replacing cDNA with water. Reactions were run on a 7500 Fast Real-Time PCR System (Applied Biosystems) using the following cycling conditions: 50 °C for 2 min, 95 °C for 10 min, followed by 40 cycles of 95 °C for 15 s and 60 °C for 1 min. Gene expression was analyzed using the ΔΔCt method with *Hprt* as the housekeeping gene.

Quantitative RT-PCR was performed in HEK-293T wild-type and SLC17A5-deficient cells as detailed above, using the following TaqMan Gene Expression Assays: *HPRT1* (Hs02800695_m1), *SLC17A5* (Exon 5–6 boundary, Hs00900587_m1), and *SLC17A5* (Exon 9–10 boundary, Hs00900590_m1). Gene expression was analyzed using the ΔΔCt method with *HPRT1* as the reference gene.

2.3. Quantitation of GSL levels in cells

Cells were pelleted and lysed in 200–300 μL of water using three freeze-thaw cycles. GSL profiling was performed as previously described [40]. Briefly, lipids were extracted overnight at 4 °C using a chloroform-methanol, followed by solid-phase extraction on C18 columns (Telos) to isolate GSLs. After elution, samples were evaporated under nitrogen at 42 °C. To facilitate downstream analysis, three-quarters of each sample underwent enzymatic digestion with recombinant ceramide glycanase (rEGCase, Genscript) to release oligosaccharides from complex GSLs, while the remaining quarter was treated with Cerezyme® (Genzyme) to hydrolyze glucosylceramide (GlcCer) and release glucose. The glycans and glucose were fluorescently labelled with anthranilic acid (2AA), and excess labeling reagent was removed using DPA-6S solid-phase extraction columns (Supelco). Purified 2AA-labelled oligosaccharides and glucose were analyzed by normal-phase high-performance liquid chromatography (HPLC). A 2AA-labelled glucose homopolymer ladder (Ludger) was used to assign glucose unit (GU) values, enabling the identification of specific GSL species based on their retention times. Quantification was performed by comparing integrated peak areas to a known 2AA-labelled BioQuant chitotriose standard (Ludger). GSL levels were normalized to total protein content, determined using the bicinchoninic acid (BCA) assay according to standard protocols.

2.4. Quantification of neuraminidase and β-hexosaminidase activities in cells

Lysosomal glycohydrolase activities in cell lysates were quantified fluorometrically using synthetic 4-methylumbelliferone (4-MU)-conjugated substrates, following established protocols [41]. Neuraminidase (Neu) activity was assessed using two assays: one measuring Neu1/3/4 activity and another specific for cytosolic Neu2, both utilizing 4-MU *N*-

acetylneuraminic acid as the substrate, with reactions incubated at 37 °C for 3.5 h. Total acid β-hexosaminidase activity (defined as HexA + HexB) was determined using 4-MU *N*-acetyl-β-D-glucosaminide, with 30-min incubation at 37 °C in a sodium citrate buffer (pH 4.5). Enzymatic reactions were terminated by adding cold 0.5 M Na_2CO_3 (pH 10.7), and liberated 4-MU fluorescence was measured using a FLUOstar OPTIMA plate reader (BMG Labtech) at an excitation wavelength of 360 nm and emission at 450 nm. Enzyme activities were calculated based on a standard curve of free 4-MU and normalized to total protein content, as determined by the bicinchoninic acid (BCA) assay.

In HEK-293T cells, NEU1/3/4 and NEU2 activities, both utilizing 4-MU *N*-acetylneuraminic acid as the substrate, were incubated at 37 °C for 3 h.

In human fibroblasts, NEU1/3/4 and NEU2 activities, both utilizing 4-MU *N*-acetylneuraminic acid as the substrate, were incubated at 37 °C for 4 h. Total acid β-hexosaminidase (defined as HexA + HexB) and HexA activities were determined using 4-MU *N*-acetyl-β-D-glucosaminide, with 30-min incubation at 37 °C in a sodium citrate buffer (pH 4.5).

2.5. Sialic acid quantification in cells

For sialic acid quantification, cell pellets were resuspended in 1 mL of water and sonicated. 25 μL of lysate was mixed with 25 μL of deuterated internal standard and either 100 μL of HPLC-grade water (for free sialic acid analysis) or 100 μL of 63 mM sulfuric acid (for total sialic acid analysis). Total sialic acid samples were incubated at 80 °C for 1 h, while free sialic acid samples were filtered using a Spin-X 0.22-μm microcentrifuge filter tube. Both free and total sialic acid were analyzed by ultra-performance liquid chromatography-tandem mass spectrometry (UPLC-MS/MS) using a Waters Acquity I-Class system coupled to a Xevo TQ-S mass spectrometer. Chromatographic separation was performed on a Waters Acquity UPLC HSS T3 C18 reverse-phase column, and detection was achieved via electrospray ionization in negative ion mode, using selected reaction monitoring. Quantification was performed by stable isotope dilution and comparison to a standard curve, with calibration curves demonstrating linearity exceeding $r^2 > 0.98$. Sialic acid concentrations were normalized to total protein content, measured using the Lowry method, and reported in nmol/mg protein.

2.6. Statistical analyses

Statistical analyses were conducted using an unpaired *t*-test or ordinary one-way ANOVA with Fisher's LSD test using GraphPad Prism (GraphPad, version 10.0.3). A two-tailed α-value for significance was set at 0.05.

3. Results

We employed a multi-pronged strategy to characterize GSL metabolism in MEFs derived from the Slc17a5-R39C/R39C knock-in and Slc17a5-KO/KO knock-out mouse models as well as SLC17A5-deficient HEK-293T cells (Fig. 1). A description of the cells used in each assay is provided in Supplementary Table 1 (MEFs) and 2 (HEK-293T cells).

3.1. Slc17a5/SLC17A5 expression and sialic acid levels in FSASD cells

qRT-PCR analysis revealed that *Slc17a5* expression in Slc17a5-KO/KO MEFs was nearly undetectable, averaging zero relative to wild-type MEFs (Figs. S1A-B). In contrast, Slc17a5-R39C/R39C MEFs exhibited a 2.34-fold increase in *Slc17a5* expression when measured with the *Slc17a5* Exon 2–3 boundary probe and a 1.15-fold increase using the *Slc17a5* Exon 10–11 boundary probe compared to wild-type MEFs (Figs. S1A-B). We observed that *SLC17A5* expression in the SLC17A5-deficient HEK-293T cells was reduced to approximately half that of wild-type cells using both the *SLC17A5* Exon 5–6 and Exon 9–10 boundary probes (Fig. S4B).

As a preliminary confirmation for the expected free sialic acid elevation in FSASD cells, UPLC-MS/MS was used to measure free and total sialic acid levels in MEFs and HEK-293T cells. Compared to wild-type MEFs, Slc17a5-R39C/R39C MEFs demonstrated an increase in free (7.7-fold) and total (1.7-fold) sialic acid levels (Figs. S3A-B), while Slc17a5-KO/KO MEFs exhibited an increase in free (47-fold) and total (3-fold) sialic acid levels (Figs. S3A-B). Next, SLC17A5-deficient HEK-

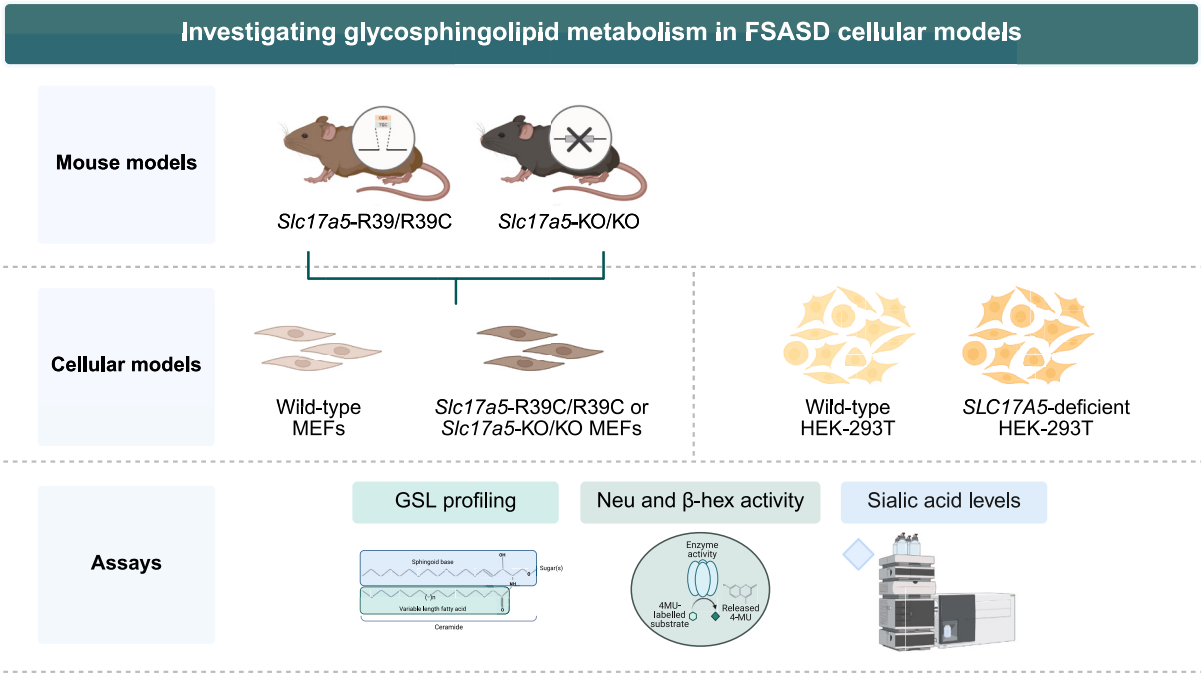

Fig. 1. Schematic overview of study. Mouse embryonic fibroblasts (MEFs) from two FSASD mouse models, as well as HEK-293T wild-type and SLC17A5-deficient cells, were used in this study. MEFs and HEK-293T cells were profiled using several assays, including quantification of glycosphingolipid (GSL) levels, neuraminidase and β-hexosaminidase activity screening, and sialic acid levels. Figure created using BioRender.com.

293T cells displayed an increase in free (12.2-fold) and total (2.2-fold) sialic acid levels (Figs. S4C). Notably, the MEFs demonstrate higher absolute levels of sialic acid compared to HEK-239T cells (Figs. S3A-B and S4C). While these findings are based on single replicates, they are consistent with the expected biochemical defect in FSASD.

3.2. GSL changes are detected in FSASD cells

Normal-phase HPLC assays revealed significant GM3 accumulation in both Slc17a5-R39C/R39C and Slc17a5-KO/KO mice compared to wild-type (Fig. 2A) whereas other detected GSL species were either reduced or unchanged (Figs. 2A and S2A). Glucosylceramide levels remained unaltered in Slc17a5-KO/KO MEFs (Fig. 2B) and were near baseline in the Slc17a5-R39C/R39C model. Representative GSL and GlcCer HPLC traces in MEFs are shown in Supplementary Figs. 2B and 2C, respectively.

In SLC17A5-deficient HEK-293T cells (Fig. S4A), a-series GSLs, including GM2, GM1a, and GD1a, were significantly reduced (Fig. 3), with the low-abundance GD3 being the only species elevated (Fig. S5A) and all other detected species remained unchanged (Figs. 3 and S5A). GlcCer levels were near the detection limit, precluding the identification of a meaningful difference in the SLC17A5-deficient HEK-293T model.

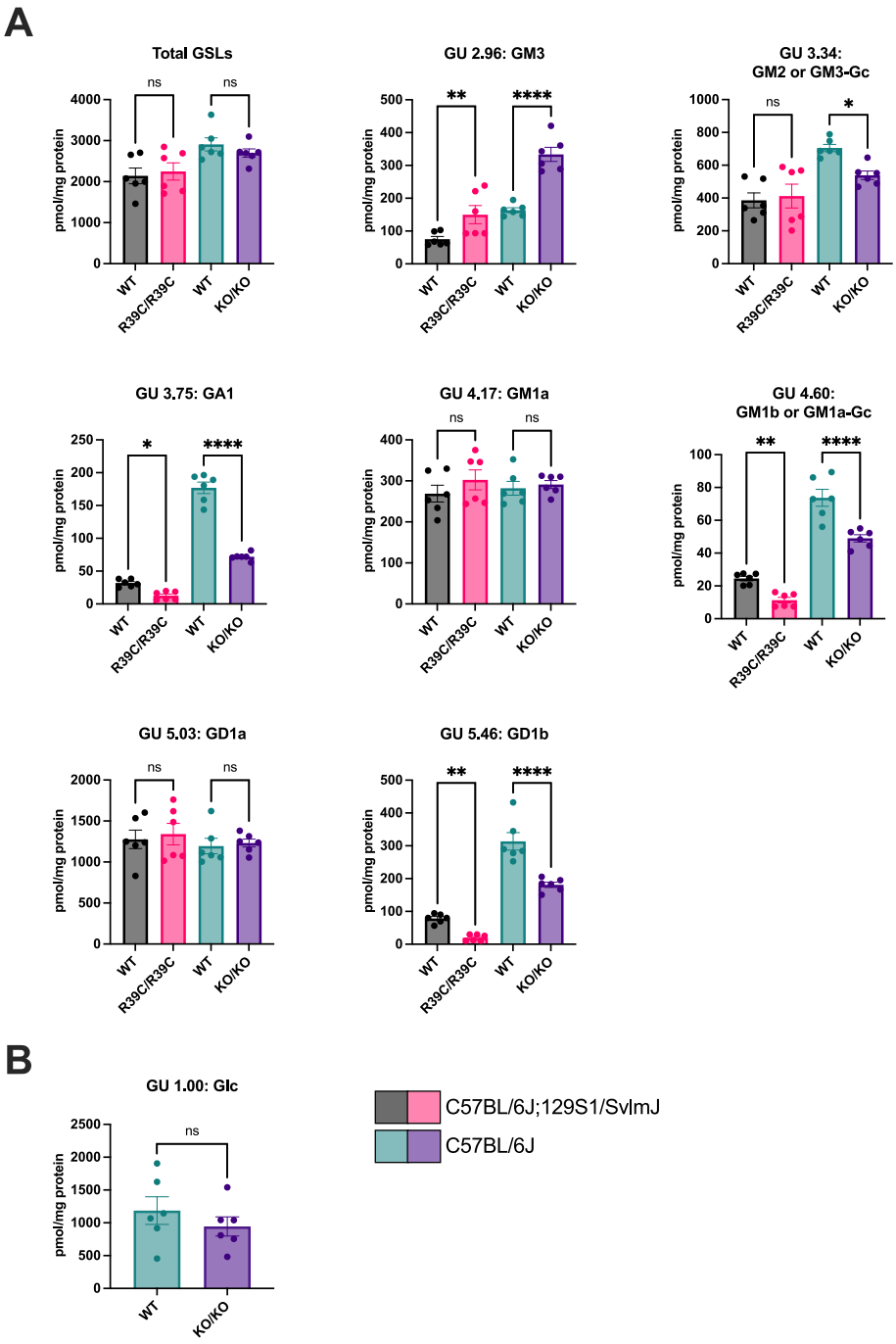

Fig. 2. Levels of total GSLs and individual GSL species in MEFs. (A) Total GSLs (addition of individual species listed in (A)) and several individual GSL species labelled with glucose units (GU) and provisional GSL assignments. (B) Glucosylceramide (Glc) levels in knock-out MEFs only. Each point denotes one replicate. Mean ± SEM; ordinary one-way ANOVA with Fisher's LSD test in (A) or unpaired *t*-test in (B) with *p*-value <0.05 (*), <0.0099 (**), <0.0001 (****), and ns = not significant.

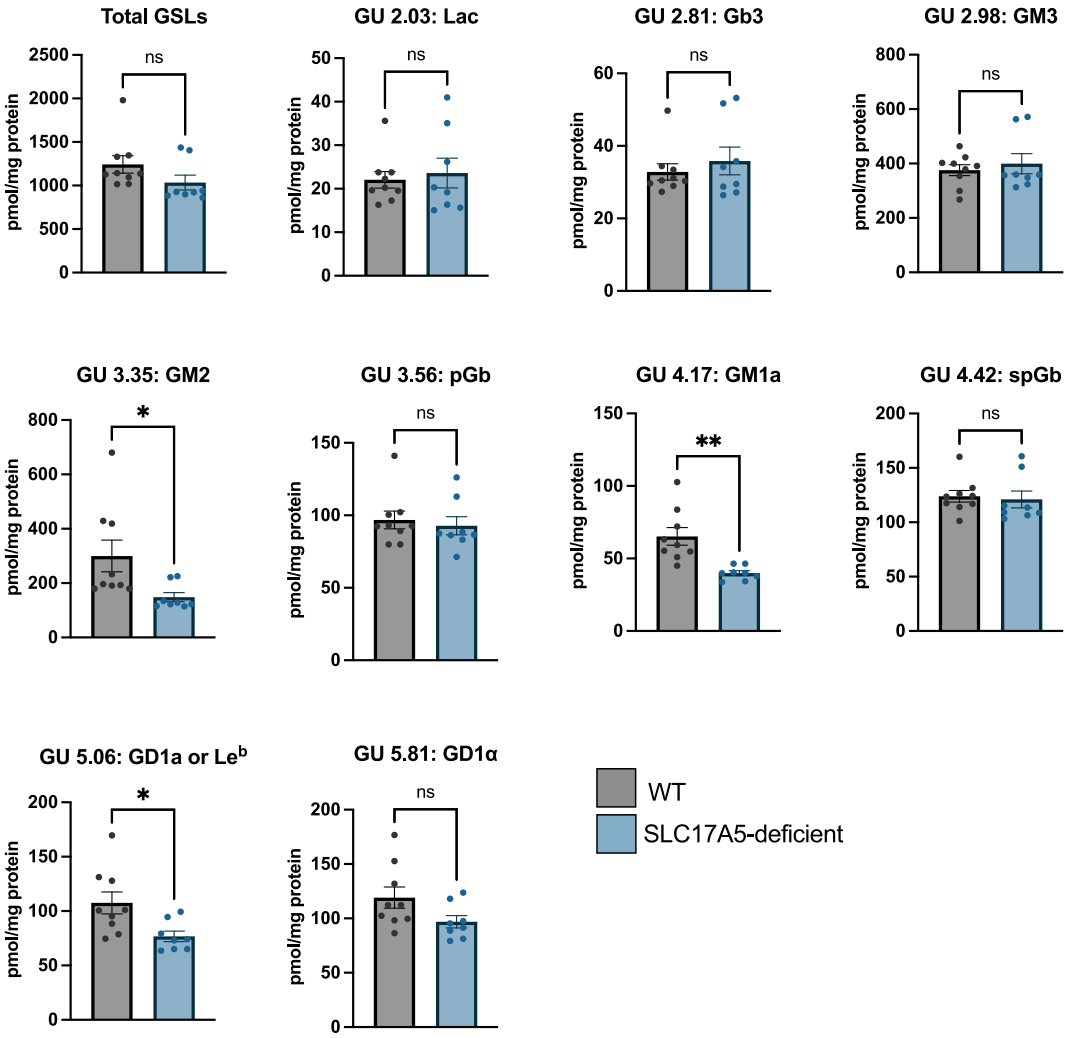

Fig. 3. Levels of total GSLs and individual GSL species in HEK-293T cells. Total GSLs (addition of individual species listed) and several individual GSL species labelled with glucose units (GU) and provisional GSL assignments. Each point denotes one replicate. Mean ± SEM; unpaired t-test with *p*-value <0.05 (*), <0.002 (**), and ns = not significant.

Representative GSL and GlcCer HPLC traces in HEK-293T cells are shown in Supplementary Figs. 5B and 5C, respectively.

Exploratory analyses in human FSASD fibroblasts (Fig. S7A) showed reduced total GSLs and decreases in GM2, GM1a, and GD1a relative to unaffected fibroblasts (Fig. S6A). Representative HPLC traces of GSLs and GlcCer from human fibroblasts are shown in Supplementary Figs. 7B and 7C, respectively.

3.3. Neuraminidase and β-hexosaminidase activity levels are altered in FSASD cells

Considering the key role of neuraminidase at the intersection of GSL and sialic acid metabolism, we quantified neuraminidase (Neu) 1/3/4 and cytosolic Neu2 activities using fluorescent 4-methylumbelliferone (4-MU) assay. Neu1/3/4 activity was increased in both Slc17a5-R39C/R39C and Slc17a5-KO/KO MEFs, with a modest elevation in Neu2 activity observed only in the Slc17a5-R39C/R39C model (Figs. 4A-B). In SLC17A5-deficient HEK-293T cells, only NEU1/3/4 activity was elevated (Fig. 4C).

Next, given the significant alteration of GM2 levels in Slc17a5-KO/KO MEFs in our study, we assessed β-hexosaminidase activity in the MEFs. The activity was significantly elevated in Slc17a5-R39C/R39C MEFs but reduced in Slc17a5-KO/KO MEFs (Figs. 4A-B). In FSASD-derived fibroblasts revealed a reduction in total β-hexosaminidase activity in FSASD patient-derived cells (Fig. S6B). A summary of the a-series GSLs (and GlcCer) along with enzyme assay results is presented in Fig. 5.

4. Discussion and limitations

4.1. Disruption of glycosphingolipid homeostasis in FSASD cells

This study offers insights into the cellular-biochemical alterations in FSASD, highlighting changes in GSL levels in in murine and human cellular models. Across all models tested, including MEFs, CRISPR-modified HEK-293T cells, and patient-derived fibroblasts, GM3 was elevated while a-series gangliosides (GM1a, GM2, GD1a) were depleted. These changes are consistent with disrupted ganglioside metabolism and recycling, potentially resulting from lysosomal sialin deficiency (schematically summarized in Fig. 6).

The selective accumulation of GM3 without corresponding increases in downstream gangliosides suggests a bottleneck in sialylation-dependent pathways, potentially due to limited CMP-sialic acid availability in the Golgi. This is supported by elevated free sialic acid levels and increased neuraminidase activity, which may further perturb sialylated glycolipid flux. Prior studies have shown that GSL expression is developmentally regulated and cell type–specific [42,43], and sialin deficiency has been linked to impaired GM3 metabolism in FSASD

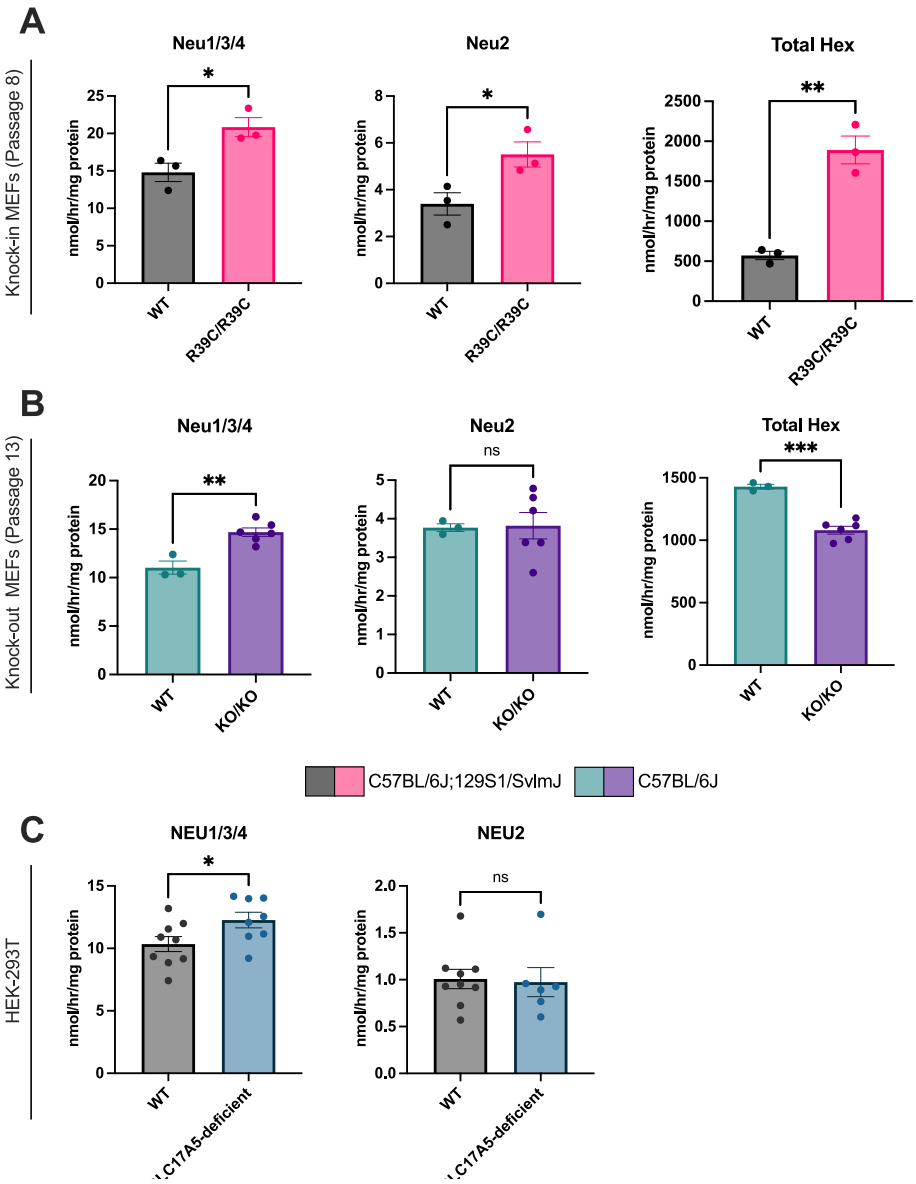

Fig. 4. Activity levels of enzymes involved in GSL catabolism in MEFs and HEK-293T cells. The following enzyme activities were measured in MEFs: neuraminidase (Neu1/3/4 and Neu2) and total β-hexosaminidase (Total Hex); (A) passage 8 cells for knock-in model and (B) passage 13 cells for knock-out model. (C) Only neuraminidase (NEU1/3/4 and NEU2) was measured in HEK-293 T cells. Activity represented as nmol per hour per mg total protein content. Each point denotes one replicate; Mean ± SEM; unpaired t-test *p*-value <0.05 (*), <0.002 (**), <0.0002 (***), and ns = not significant.

fibroblasts [19]. While total GSL levels in MEFs remained unchanged, the altered profile—characterized by increased GM3 and reduced downstream a-series GSLs—indicates that reduced sialin activity selectively impacts specific ganglioside species rather than global GSL levels.

Furthermore, in SLC17A5-deficient HEK-293T cells and human fibroblasts, we observed a decrease in GM2, similar to that seen in Slc17a5-KO/KO MEFs in our study, along with a reduction in other a-series GSLs, including GM1a and GD1a. These findings suggest a potential defect in the biosynthesis or regulation of a-series GSLs in sialin-deficient cells.

In Slc17a5-R39C/R39C MEFs and SLC17A5-deficient HEK-293T cells, glucosylceramide levels were at baseline (undetectable). However, it remains unclear whether this glucosylceramide pool was depleted through conversion to glucosylsphingosine in these models.

4.2. *Neuraminidase activity levels are altered in FSASD cells*

Neuraminidases play a critical role in the turnover of sialylated glycoconjugates, including gangliosides [44]. Free sialic acid has also been reported to act as a competitive inhibitor of lysosomal neuraminidases [13,45], suggesting that dysregulated sialic acid levels could disrupt normal catabolic processes. The observed increase in neuraminidase activity across multiple sialin-deficient models likely reflects a compensatory mechanism in response to impaired ganglioside degradation. This upregulation may contribute to the altered GSL profiles and points to broader disruptions in lysosomal homeostasis.

One possible explanation for this increased activity is that impaired efflux of free sialic acid from lysosomes—due to loss of sialin function—leads to both substrate accumulation and secondary dysregulation of lysosomal pH. This may create a lysosomal milieu that enhances neuraminidase activity either directly, via changes in enzyme stability or trafficking, or indirectly, through transcriptional feedback loops. Interestingly, reduced β-hexosaminidase activity observed in both Slc17a5-KO/KO MEFs and patient fibroblasts suggests an additional facet of lysosomal dysfunction and may serve as a potential biomarker of more severe sialin deficiency. Notably, loss of Neu3 activity in the mouse

A

	Slc17a5-R39C/R39C MEFs	Slc17a5-KO/KO MEFs	SLC17A5-deficient HEK-293T
Total GSLs	=	=	=
GU 2.96-2.98: *GM3*	↑	↑	=
GU 3.34-3.35: *GM2*	=	↓	↓
GU 4.17: *GM1a*	=	=	↓
GU 5.03-5.06: *GD1a*	=	=	↓
GU 1.00: *GlcCer*	NA*	=	NA*

B

	Slc17a5-R39C/R39C MEFs	Slc17a5-KO/KO MEFs	SLC17A5-deficient HEK-293T
Neuraminidase 1/3/4	↑	↑	↑
Neuraminidase 2	↑	=	=
β-hexosaminidase	↑	↓	NM

Fig. 5. Summary of (a-series) GSLs and GlcCer in addition to enzyme activity levels across each cellular model. Comparison of cells harboring *Slc17a5/SLC17A5* mutations versus respective wild-type cells. Up arrows denote significantly elevated GSL species or enzyme activities, while down arrows indicate significantly decreased levels or activities. An equal sign signifies no significant difference between wild-type and mutant groups. NA* indicates that the GlcCer was assayed but was not detectable above baseline. NM (not measured) means that no additional enzyme activity assays were conducted for that cell type.

brain has been reported to exacerbate GM1 ganglioside accumulation in a murine model of GM1 gangliosidosis, another lysosomal storage disorder [46].

4.3. Intersection of sialic acid and ganglioside metabolism

We postulate that in the FSASD cell models examined, lysosomal sequestration of free sialic acid contributes to glycolipid hyposialylation by disrupting intracellular sialic acid homeostasis. This disruption likely impairs the efficient recycling and reutilization of sialic acid for biosynthetic processes, particularly for the de novo synthesis of CMP-sialic acid, the activated donor required for sialyltransferase-mediated glycosylation. Since glycolipid sialylation primarily occurs in the Golgi apparatus and is critically dependent on a constant supply of CMP-sialic acid [47], any reduction in the availability of this substrate may compromise the biosynthesis of gangliosides, which depend on terminal sialylation.

4.4. Limitations and future studies

We acknowledge limitations in this study. The Slc17a5-R39C/R39C and Slc17a5-KO/KO mice differ in genetic background, which may affect GSL and GSL glycohydrolase levels [48]. The Slc17a5-KO/KO MEFs were obtained and analyzed at a higher passage number than Slc17a5-R39C/R39C MEFs, possibly influencing cellular behavior. Despite extensive testing, we were unable to quantify sialin protein due to lack of a reliable commercially available antibody (extensively tested, data not shown). Additionally, only Neu5Ac was measured by UPLC-MS/MS; although validated assays for Neu5Gc exist, our reliance on a clinical assay limited access to these methods, preventing Neu5Gc measurement. Future research should aim to delineate the contribution of Neu5Gc in the FSASD mouse cellular models.

MEFs comprise diverse subpopulations [49] and rapidly undergo senescence due to oxidative stress following isolation and passaging [50,51]. Cell sorting to isolate specific MEF subpopulations could help address this heterogeneity. Additionally, the impact of senescence on GSL levels and flux, particularly in the context of sialin deficiency, remains unclear. Utilizing immortalized MEFs [52] or neuronal cell models could provide more stable and physiologically relevant model for investigating these effects.

To evaluate the potential of these cellular models for therapeutic screening, future studies should determine whether the observed biochemical phenotypes—elevated neuraminidase 1/3/4 activity, altered GSL abundance, and increased levels of free sialic acid—can be reversed with *SLC17A5* gene correction. Future work should also prioritize flux-based assays to differentiate between static accumulation and dynamic processing defects. Collectively, these findings highlight the utility of FSASD mouse embryonic fibroblasts and SLC17A5-deficient HEK-293T cells as complementary model systems to patient-derived human fibroblasts for advancing mechanistic studies of FSASD pathogenesis.

Supplementary data to this article can be found online at https://doi.org/10.1016/j.ymgmr.2025.101275.

CRediT authorship contribution statement

Marya S. Sabir: Writing – review & editing, Writing – original draft, Visualization, Investigation, Formal analysis, Conceptualization. **Kostantin Dobrenis:** Writing – review & editing, Resources. **Allisandra K. Rha:** Writing – review & editing, Investigation. **Laura Pollard:** Writing – review & editing, Investigation, Funding acquisition. **Petcharat Leoyklang:** Writing – review & editing, Investigation. **Mariah Marrero:** Writing – review & editing, Investigation. **Carla Ciccone:** Writing – review & editing, Investigation. **Mary E. Hackbarth:** Writing – review & editing, Investigation. **Marjan Huizing:** Writing – review & editing, Supervision. **Raymond Y. Wang:** Writing – review & editing, Resources, Funding acquisition. **William A. Gahl:** Writing – review & editing, Supervision, Funding acquisition. **Frances M. Platt:** Writing – review & editing, Supervision, Resources, Funding acquisition, Conceptualization. **May Christine V. Malicdan:** Writing – review & editing, Supervision, Resources, Conceptualization.

Ethics statement

Animal care, procedures, and euthanasia were conducted in accordance with the guidelines set forth by the Institutional Animal Care and Use Committees (IACUC) of the NIH National Human Genome Research Institute for the knock-in mouse model and of the Albert Einstein College of Medicine for the knock-out mouse model. The animals were maintained and cared for under an ACUC approved animal study protocol (G-14-5). The FSASD patient-derived fibroblast cell line was established from a donor enrolled in NIH protocol 14-HG-0071 (NCT02089789), conducted with approval from the Institutional Review Board of the NIH National Human Genome Research Institute.

Funding

This work was supported in part by the National Institutes of Health Intramural Research Program (IRP) of the National Human Genome Research Institute and IRP of other institutes contributing to the NIH Undiagnosed Diseases Program. The contributions of the NIH authors are considered works of the U.S. government. The findings and conclusions presented in this paper are those of the authors and do not necessarily reflect the views of the NIH or the U.S. Department of Health and Human Services. MSS received a graduate fellowship from the National Institutes of Health Oxford-Cambridge Scholars Program. AKR and RYW were supported by the Campbell Foundation of Caring and Larry and Helen Hoag Foundation. The Salla Treatment and Research

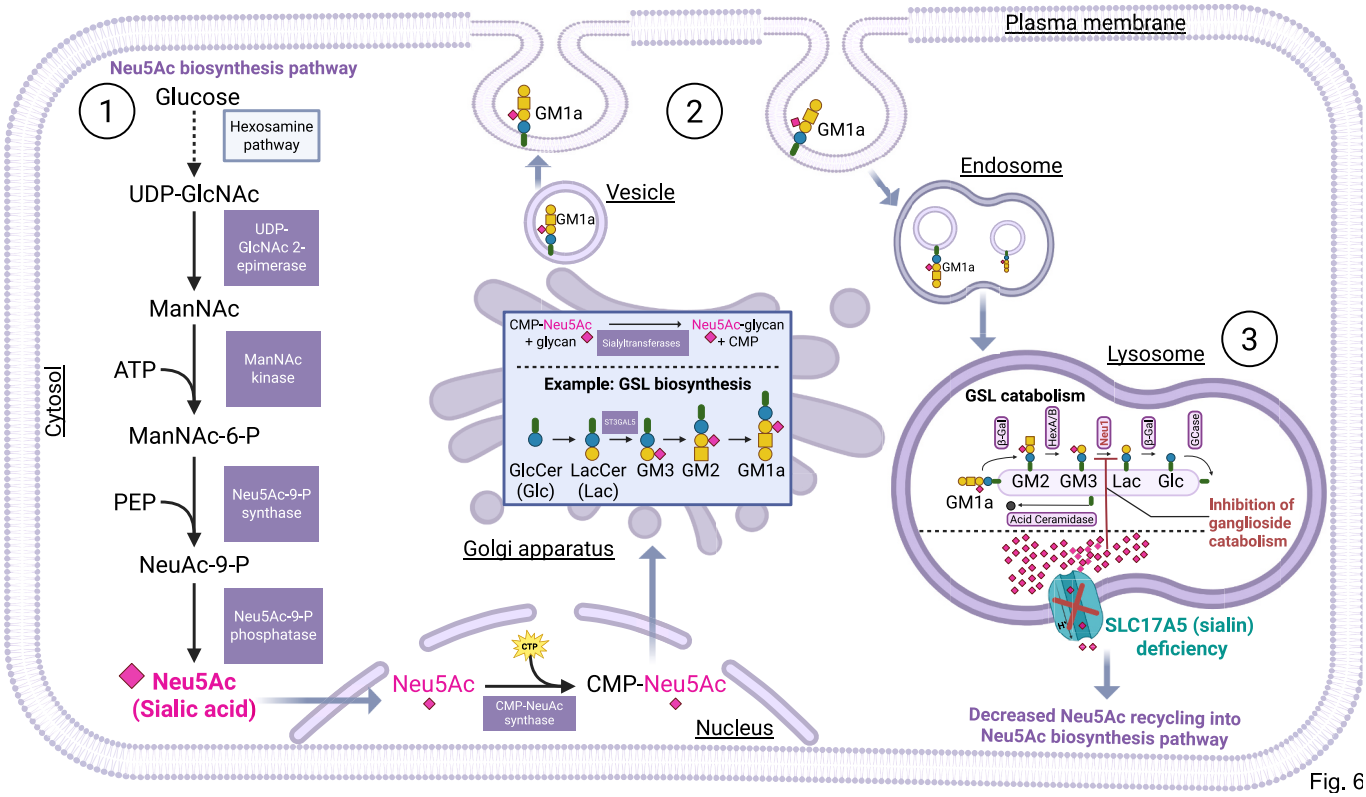

Fig. 6

Fig. 6. Schematic overview of the intersection between sialic acid and ganglioside metabolism in the context of SLC17A5 (sialin) deficiency. (1) Sialic acid (Neu5Ac) is synthesized from glucose in the cytosol through sequential enzymatic reactions and subsequently activated in the nucleus to CMP-Neu5Ac. CMP-Neu5Ac is then transported into the Golgi by the CMP-sialic acid transporter SLC35A1, where sialylstransferases use it to sialylate glycoproteins and glycolipids. In this figure, GM1a synthesis is shown to illustrate the role of sialic acid in glycolipid biosynthesis. (2) Newly synthesized glycosphingolipids (GSLs, including gangliosides) are trafficked via vesicles to the plasma membrane. After functional turnover, GSLs (e.g., GM1a) are endocytosed and delivered to the lysosome. (3) In lysosomes, gangliosides in intraluminal vesicles are stepwise degraded by glycosidases, including neuraminidases (e.g., Neu1) which releases free Neu5Ac. Under normal conditions, SLC17A5 (sialin) exports free Neu5Ac from lysosomes to the cytosol, a process that contributes to the sialic acid salvage (recycling) pathway. Free Neu5Ac then is either reactivated to CMP-Neu5Ac to support ongoing sialylation, or cleaved to ManNAc + pyruvate by the cytosolic enzyme *N*-acetylneuraminate pyruvate lyase (NPL), with ManNAc re-entering the de novo sialic acid biosynthesis. In FSASD, loss of sialin function impairs lysosomal efflux of free Neu5Ac, causing intralysosomal accumulation and curtailing the salvage contribution to the CMP-Neu5Ac pool. This Neu5Ac accumulation has been reported to inhibit neuraminidases involved in ganglioside catabolism [13,45], resulting in secondary gangliosides storage. Although global cellular sialylation can often be maintained by de novo synthesis, reduced salvage likely can, in some contexts, limit sialylation of specific substrates under high demand. Created with BioRender.com.

Foundation awarded a grant to Greenwood Genetic Center (LP) for sialic acid quantification. The sponsors did not have a role in the study design, collection, analysis and interpretation of data, writing of the report, or decision to submit the article for publication.

Declaration of competing interest

The authors declare no conflicts of interest.

Acknowledgements

We would like to express our gratitude to the NIH NHGRI Mouse Transgenic Core for their assistance in generating the Slc17a5-R39C/R39C mouse model, from which the knock-in MEFs were isolated. We would like to thank Chloe Christensen (Children's Hospital of Orange County) for her assistance with shipment of samples. The authors gratefully acknowledge Lynne Wolfe (NIH/NHGRI) for collecting fibroblast samples from patient CDG1121 as part of NIH protocol 14-HG-0071 (NCT02089789).

Data availability

Data will be made available on reasonable request from corresponding authors.

References

[1] F.W. Verheijen, et al., A new gene, encoding an anion transporter, is mutated in sialic acid storage diseases, Nat. Genet. 23 (4) (1999) 462–465.
[2] D. Adams, M. Wasserstein, Free sialic acid storage disorders, in: M.P. Adam, et al. (Eds.), GeneReviews((R)), 2020. Seattle (WA).
[3] H.J. Blom, et al., Defective glucuronic acid transport from lysosomes of infantile free sialic acid storage disease fibroblasts, Biochem. J. 268 (3) (1990) 621–625.
[4] P. Courville, M. Quick, R.J. Reimer, Structure-function studies of the SLC17 transporter sialin identify crucial residues and substrate-induced conformational changes, J. Biol. Chem. 285 (25) (2010) 19316–19323.
[5] P. Morin, C. Sagne, B. Gasnier, Functional characterization of wild-type and mutant human sialin, EMBO J. 23 (23) (2004) 4560–4570.
[6] N. Pietrancosta, et al., Successful prediction of substrate-binding pocket in SLC17 transporter sialin, J. Biol. Chem. 287 (14) (2012) 11489–11497.
[7] M. Huizing, et al., Free sialic acid storage disorder: Progress and promise, Neurosci. Lett. 755 (2021) 135896.
[8] N. Aula, et al., The spectrum of SLC17A5-gene mutations resulting in free sialic acid-storage diseases indicates some genotype-phenotype correlation, Am. J. Hum. Genet. 67 (4) (2000) 832–840.
[9] R. Barmherzig, et al., A new patient with intermediate severe Salla disease with Hypomyelination: a literature review for Salla disease, Pediatr. Neurol. 74 (2017) 87–91 e2.
[10] R. Kleta, et al., Biochemical and molecular analyses of infantile free sialic acid storage disease in north American children, Am. J. Med. Genet. A 120A (1) (2003) 28–33.
[11] T. Varho, et al., Central and peripheral nervous system dysfunction in the clinical variation of Salla disease, Neurology 55 (1) (2000) 99–104.
[12] M. Pitto, et al., Impairment of ganglioside metabolism in cultured fibroblasts from Salla patients, Clin. Chim. Acta 247 (1–2) (1996) 143–157.

[13] K. Mendla, M. Cantz, Specificity studies on the oligosaccharide neuraminidase of human fibroblasts, Biochem. J. 218 (2) (1984) 625–628.
[14] M. Renlund, et al., Free N-acetylneuraminic acid in tissues in Salla disease and the enzymes involved in its metabolism, Eur. J. Biochem. 130 (1) (1983) 39–45.
[15] A. Fois, et al., Free sialic acid storage disease. A new Italian case, Eur. J. Pediatr. 146 (2) (1987) 195–198.
[16] J. Baumkotter, et al., N-Acetylneuraminic acid storage disease, Hum. Genet. 71 (2) (1985) 155–159.
[17] C. Nakano, et al., A Japanese case of infantile sialic acid storage disease, Brain Dev. 18 (2) (1996) 153–156.
[18] K. Mendla, et al., Defective lysosomal release of glycoprotein-derived sialic acid in fibroblasts from patients with sialic acid storage disease, Biochem. J. 250 (1) (1988) 261–267.
[19] V. Chigorno, G. Tettamanti, S. Sonnino, Metabolic processing of gangliosides by normal and Salla human fibroblasts in culture. A study performed by administering radioactive GM3 ganglioside, J. Biol. Chem. 271 (36) (1996) 21738–21744.
[20] L.M. Prolo, H. Vogel, R.J. Reimer, The lysosomal sialic acid transporter sialin is required for normal CNS myelination, J. Neurosci. 29 (49) (2009) 15355–15365.
[21] S. Stroobants, et al., Progressive leukoencephalopathy impairs neurobehavioral development in sialin-deficient mice, Exp. Neurol. 291 (2017) 106–119.
[22] M.S. Sabir, et al., A novel experimental mouse model to investigate a free sialic acid storage disorder (Salla disease), Mol. Genet. Metab. 135 (2) (2022) S107.
[23] M.E. Hackbarth, et al., A Mouse Model of Free Sialic Acid Storage Disorder: Hypomyelinating Leukodystrophy and Purkinje Cell Degeneration, 2025. Unpublished Results.
[24] Y. Chen, et al., Proteomic and phosphoproteomic characterisation of primary mouse embryonic fibroblasts, Proteomics 24 (7) (2024) 2300267.
[25] I. Saitoh, et al., Choice of feeders is important when first establishing iPSCs derived from primarily cultured human deciduous tooth dental pulp cells, Cell Med. 8 (1–2) (2015) 9–23.
[26] C. Zhuo, et al., Proteomics analysis of autophagy-deficient Atg7−/− MEFs reveals a close relationship between F-actin and autophagy, Biochem. Biophys. Res. Commun. 437 (3) (2013) 482–488.
[27] H. Ren, G. Wang, Autophagy and lysosome storage disorders, Adv. Exp. Med. Biol. 1207 (2020) 87–102.
[28] G. Lunghi, et al., Regulation of signal transduction by gangliosides in lipid rafts: focus on GM3-IR and GM1-TrkA interactions, FEBS Lett. 596 (24) (2022) 3124–3132.
[29] R.L. Schnaar, Gangliosides as Siglec ligands, Glycoconj. J. 40 (2) (2023) 159–167.
[30] K.I. Inamori, J.I. Inokuchi, When ganglioside pathways go awry: congenital disorders and experimental insights, J. Hum. Genet. (2025).
[31] A. Janez Pedrayes, et al., Glycosphingolipids in congenital disorders of glycosylation (CDG), Mol. Genet. Metab. 142 (1) (2024) 108434.
[32] K.L. Wallom, et al., Glycosphingolipid metabolism and its role in ageing and Parkinson's disease, Glycoconj. J. 39 (1) (2022) 39–53.
[33] F.M. Platt, The expanding boundaries of sphingolipid lysosomal storage diseases; insights from Niemann-pick disease type C, Biochem. Soc. Trans. 51 (5) (2023) 1777–1787.
[34] A.E. Ryckman, I. Brockhausen, J.S. Walia, Metabolism of glycosphingolipids and their role in the pathophysiology of lysosomal storage disorders, Int. J. Mol. Sci. 21 (18) (2020).
[35] B. Breiden, K. Sandhoff, Lysosomal glycosphingolipid storage diseases, Annu. Rev. Biochem. 88 (2019) 461–485.
[36] B. Breiden, K. Sandhoff, Mechanism of secondary ganglioside and lipid accumulation in lysosomal disease, Int. J. Mol. Sci. 21 (7) (2020).
[37] M.S. Sabir, et al., Changes in glycosphingolipid levels in plasma and cerebrospinal fluid of individuals with lysosomal free sialic acid storage disorder, Rare 3 (2025) 100065.
[38] A.V. Pshezhetsky, M. Ashmarina, Keeping it trim: roles of neuraminidases in CNS function, Glycoconj. J. 35 (4) (2018) 375–386.
[39] M. Wendeler, K. Sandhoff, Hexosaminidase assays, Glycoconj. J. 26 (8) (2009) 945–952.
[40] D.A. Priestman, et al., Analysis of Glycosphingolipids from Cell Lines, 2024 protocols.io.
[41] M. Huebecker, et al., Reduced sphingolipid hydrolase activities, substrate accumulation and ganglioside decline in Parkinson's disease, Mol. Neurodegener. 14 (1) (2019) 40.
[42] R.K. Yu, Development regulation of ganglioside metabolism, Prog. Brain Res. 101 (1994) 31–44.
[43] R.K. Yu, et al., Developmental changes in ganglioside composition and synthesis in embryonic rat brain, J. Neurochem. 50 (6) (1988) 1825–1829.
[44] S. Okun, A. Peek, S.A. Igdoura, Neuraminidase 4 (NEU4): new biological and physiological player, Glycobiology 33 (3) (2023) 182–187.
[45] T. Miyagi, K. Yamaguchi, Mammalian sialidases: physiological and pathological roles in cellular functions, Glycobiology 22 (7) (2012) 880–896.
[46] M.L. Allende, et al., Sialidase NEU3 action on GM1 ganglioside is neuroprotective in GM1 gangliosidosis, J. Lipid Res. 64 (12) (2023) 100463.
[47] E. Nji, et al., Structural basis for the delivery of activated sialic acid into Golgi for sialyation, Nat. Struct. Mol. Biol. 26 (6) (2019) 415–423.
[48] A. Duran, et al., A mouse systems genetics approach reveals common and uncommon genetic modifiers of hepatic lysosomal enzyme activities and glycosphingolipids, Int. J. Mol. Sci. 24 (5) (2023).
[49] P.K. Singhal, et al., Mouse embryonic fibroblasts exhibit extensive developmental and phenotypic diversity, Proc. Natl. Acad. Sci. USA 113 (1) (2016) 122–127.
[50] R.A. Busuttil, et al., Oxygen accelerates the accumulation of mutations during the senescence and immortalization of murine cells in culture, Aging Cell 2 (6) (2003) 287–294.
[51] S. Parrinello, et al., Oxygen sensitivity severely limits the replicative lifespan of murine fibroblasts, Nat. Cell Biol. 5 (8) (2003) 741–747.
[52] S. Srinivasan, H.H. Ho, An efficient method for immortalizing mouse embryonic fibroblasts by CRISPR-mediated deletion of the Tp53 gene, Bio-Protoc. 15 (2) (2025) e5159.